Comparison of Lead Zirconate Titanate Properties between the Pressing Process and the Gel Casting Process by using Ethylene Glycol Diglycidyl Ether (EGDGE) Epoxy Resin as a Gelling Agent

Tanikan Thongchai

Faculty of Engineering, Department of Industrial Engineering, Naresuan University, Phitsanulok, 65000, Thailand

Corresponding author. E-mail address: tanikant@nu.ac.th

Abstract

Gel casting has been widely developed during the past ten years due to its applicability in the complex shape fabrication of small ceramic products such as transducers and sensors, and this process provides a low-cost manufacturing route. The purpose of this research is to focus on the PZT properties resulting from the pressing and gel casting processes. In the pressing process, a soft PZT 5H powder was pressed using an Instron testing machine under 90 MPa. In the gel casting process, the ethylene glycol diglycidyl ether (EGDGE) epoxy monomer and a solution of an ammonium salt of an acrylic polymer in water (NH_4PAA) were utilised as a gelling agent and dispersant, respectively. The results showed that the viscosity of the PZT was minimised by adding 1.2 wt% of the dispersant. The highest green strength of approximately 35 MPa was found from the pressed sample. In the gel casting process, at 40 wt% EGDGE resin content and 46 vol% solids loading provided the highest green strength of approximately 30 MPa. The PZT samples from both processes were sintered at 1,200 $^{\circ}$C. The sample from the pressing process provided the highest values of d_{33}, k_p and ε_r of approximately 590 pC/N, 0.62, and 2,875, respectively; while the PZT samples fabricated from a gel casting slurry incorporating a 40 wt% EGDGE resin and 46 vol% solids loading provided d_{33}, k_p and ε_r values of approximately 575 pC/N, 0.6, and 2800, respectively. The results indicated that the desired properties of the pressed PZT sintered samples were slightly higher than those of the properties of the PZT gel cast samples.

Keywords: PZT, Piezoelectric, Dielectric, EGDGE Epoxy Resin, Gel Casting

Introduction

Piezoelectricity is a phenomenon that can be described as the interaction between the electrical and mechanical properties of some materials. The direct piezoelectric effect is defined as the polarisation generated by the application of a mechanical stress, which is exploited in generators or sensor applications. Vice versa, when a piezoelectric material is subjected to an applied electrical field, strain is induced. This phenomenon is known as the converse or indirect effect, which is used in motor applications (Moulson & Herbert, 2003; Patranabi, 2003; Sinclair, 2001). The most common piezoelectric material used is lead zirconate titanate ($PbZr_xTi_{1-x}O_3$) perovskite ceramic. Lead zirconate titanate based materials dominate the piezoelectric material market, including piezoelectric materials for sensors, ceramic capacitors, ultrasonic non-destructive testing, and medical ultrasound applications. Above the Curie temperature, PZT exhibits cubic symmetry with no piezoelectricity as the charges in the unit cell cancel each other, giving a zero net dipole; while below the Curie point, the lattice structure becomes distorted along the <100> or <111> directions. In the resultant tetragonal and rhombohedral unit cells, Ti and Zr atoms are slightly off-centre; therefore, net dipoles are developed. For PZT, the Curie temperature can be tuned by changing the composition, more specifically, the mole ratio of Zr and Ti, i.e. the x value in the general formula. It is interesting to note that the transition boundary between the tetragonal and rhombohedral phases, known as the morphotropic phase boundary

(MPB), is nearly independent of temperature. PZT ceramics show the most beneficial piezoelectric properties for compositions near the MPB (x = 0.52 at room temperature) due to the coexistence of the two ferroelectric phases in this region.

Gel casting is a colloidal ceramic process that improves ceramic reliability. It is a useful technique for producing ceramic parts with complex shapes and homogeneous ceramic bodies. This process also inherently provides a low-cost manufacturing route as well as the capability of near-net-shape fabrication of small ceramic products, including piezoelectric materials for ultrasound transducer applications (Liu, Huang, & Yang, 2002; Yang, Yu, & Huang, 2011). The principle of this process was originally developed in the Oak Ridge National Laboratory (Oak Ridge, TN, USA) by Omatete, Janney, and Strehlow during the 1980s. It is based on a synthetic idea originated from conventional ceramics and from polymer chemistry (Janney et al., 1998; Omatete, Janney, & Strehlow, 1991). The most common gel casting process is based on dispersing ceramic powders in a solution containing a monomer, crosslinker, initiator and catalyst in order to form a castable slurry with a high solids loading, and then the slurry is poured into a mould and solidified in situ to form a green body having the shape of the mould. The gelled part is removed from the mould after gelation, and then dried to remove the solvent, followed by the binder removal and sintering stages that are applicable to other ceramic processing routes. Therefore, the small ceramic particles can be solidified in order to form high green strength and uniform ceramic bodies with fewer imperfections in the microstructure (Yang et al., 2011).

The heart of the gel casting process is the irreversible formation of a gel, which allows particles to retain their dispersed state and gives significant strength to the gelled green body. For the original study, Acrylamide (AM) and N,N'-Methylenebisacrylamide (MBAM) were used as a monomer and crosslinker, respectively. However, polymerisation of this monomer is a free-radical reaction that is easily inhibited by oxygen, resulting in the surface-exfoliation phenomenon of the green bodies (Dong, Mao, Zhang, & Liu, 2009), and also, the industry is unwilling to use the acrylamide system due to its neurotoxicity (Janney et al., 1998).

A water-soluble epoxy resin and hardener system was recently used in an alumina and SiC gel casting process by Mao, Shimai, Wang, Dong, and Jin (2009). The epoxide group of epoxy resin and the active hydrogen of amine is a nucleophilic addition reaction instead of a free radical reaction. Therefore, using epoxy resin as a gel former can avoid oxygen inhibition (Mao et al., 2009). Sorbitol polyglycidyl ether (SPGE) was studied as a gelling agent and 3,3'-Iminodipropylamine was utilised as an amine hardener. The results showed that the process can be carried out in air without any surface problems. However, this epoxy resin is difficult to dissolve in water and the slurry has a relatively high viscosity. To overcome the drawbacks of the SPGE-based system, the development of a new system was necessary. Ethylene glycol diglycidyl ether (EGDGE) has been studied in various works, and it was also found to be an excellent alternative to SPGE due to its ability to form high-strength dried gel cast bodies (Mao et al., 2009; Olhero, Garcia-Gancedo, Button, Alves, & Ferreira, 2012; Mao, Shimai, Dong, & Wang, 2007, 2008). In this work, PZT and ethylene glycol diglycidyl ether (EGDGE) have been selected for the preparation of gel casting slurries for the fabrication of bulk gel casting samples and an investigation of their properties compared with samples from the pressing process.

Method and Materials

A commercial soft PZT 5H-TRS powder from TRS Technologies, USA with the MPB composition $[Pb(Zr_{0.52}Ti_{0.48})O_3]$ (High Performance soft PZT, 2017) with a density of 7.95 g/cm^3 was used. The PZT as-received powder was vibro-milled for 48 hrs and dried, and the average particle size was reduced to approximately 1.2 μm with an almost unimodal distribution, indicating that the agglomerates had been broken down. For fabrication of the pressed powder, the soft PZT 5H powder was pressed using an Instron testing machine under 90 MPa and a stainless steel die with a 13-mm diameter. In the gel casting process, each batch size of slurry was prepared with approximately 40 g of ethylene glycol diglycidyl ether (EGDGE) epoxy resin (EX-810, Nagase ChemteX Corporation, Japan) with an epoxy equivalent weight of 113 g/mol and studied from 10 – 40 wt%. Bis(3-aminopropyl)amine with a molecular weight of 131.22 g/mol was used as a hardener (the chemical structures of which are shown in Figure 1). In order to complete the reaction between the epoxy resin and the amine hardener, 1 g of epoxy resin per 0.1 g of amine hardener was used. The EGDGE was dissolved in distilled water. A solution of an ammonium salt of an acrylic polymer in water (NH_4PAA), or Dispex AA4040, was utilised as a dispersing agent and added followed by the addition of the PZT powder. The powder addition was separated into four stages in the pattern 1/2, 1/4, 1/8 and 1/8 of the required amount, and the slurries were milled for 20 minutes using a magnetic stirrer in order to achieve a high solids loading and low viscosity, well-mixed slurry, followed by the addition of Bis(3-aminopropyl)amine hardener. The slurries were degassed in a vacuum chamber for 2 minutes and then were cast into the mould. Samples were dried at room temperature for 24 hours followed by another 48 hours in an oven at 50 $^\circ$C.

Bulk PZT pressed and gel casting samples were characterised by density, strength and microstructure and then were sintered in a furnace. The process of the organic burnout was separated into two steps. Firstly, the samples were heated from 40 to 250 $^\circ$C at 1 $^\circ$C/minute and kept at 250 $^\circ$C for 60 minutes. Secondly, the temperature was increased from 250 $^\circ$C to 400 $^\circ$C at the same heating rate, followed by maintenance of this temperature for 1 hour. After that, the ramp rate was changed to 5 $^\circ$C/minute to reach the sintering temperature of 1200 $^\circ$C, which was maintained for 1 hour, followed by cooling to 40 $^\circ$C at a rate of 5 $^\circ$C/minute. Density and flexural strength were measured based on Archimedes' method by using a balance (model R300S, Sartorius GMBH Gottingen, Germany) and Instron testing machine (Buckinghamshire, UK), respectively. Microstructures were observed by using a Scanning Electron Microscope (model JSM6060, Jeol, Tokyo, Japan). The Piezoelectric charge coefficient (d_{33}) and planar coupling coefficient (k_p), as well as the relative permittivity (ε_r) and dielectric loss, were studied with a frequency range of 40 Hz – 110 MHz (Agilent 4294A impedance analyser, Agilent Ltd, UK).

(a)   (b)

Figure 1 Chemical structure for the (a) epoxide resin: $C_8H_{14}O_4$, EGDGE; (b) hardener: $C_6H_{17}N_3$, Bis(3-aminopropyl)amine

<div align="center">

Results

</div>

Particle size and crystalline material structure analysis

The particle size distribution of the as-received powder is shown in Figure 2(a), which presents a bimodal distribution with peaks centred at 26.95 μm and 2.60 μm, respectively, indicating significant agglomeration. After vibro-milling for 48 hrs the average particle size was reduced to approximately 1.2 μm with an almost unimodal distribution, indicating the agglomerates had been broken down, as can be seen in Figure 2(b). Figure 3(a) shows the SEM micrograph of the as-received powder, in which the powder morphology has doughnut-shaped granules from spray drying. The agglomeration can be seen with a broad range of powder size from less than 5 μm to over 30 μm, as the large agglomerates were broken down after the powder was vibro-milled for 48 hrs, leading to the fine particles as seen in Figure 3(b).
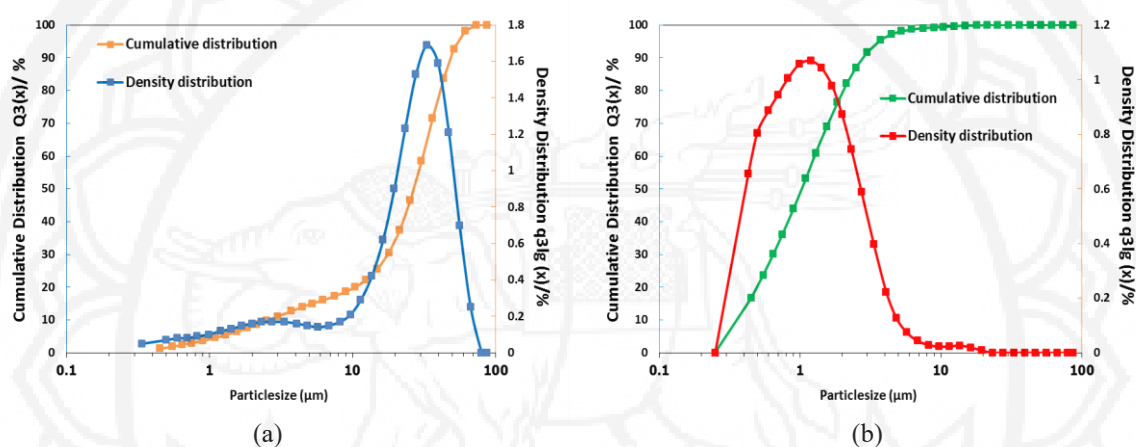

(a)   (b)

Figure 2 Particle size distribution of PZT 5H powder: (a) as-received and (b) after vibro-milling for 48 hrs

(a)   (b)

Figure 3 SEM micrographs of PZT 5H powder: (a) as-received and (b) after vibro-milling for 48 hrs

In the XRD patterns of the as-received PZT powder and discs sintered at 1200 $^\circ$C, both XRD patterns can be indexed as a tetragonal perovskite phase, as the patterns of the as-received powder matched the ICSD code: 86136 (Corker, Glazer, Whatmore, Stallard, & Fauth, 1998), with the pattern being similar to Pb(Zr$_{0.52}$Ti$_{0.48}$)O$_3$.
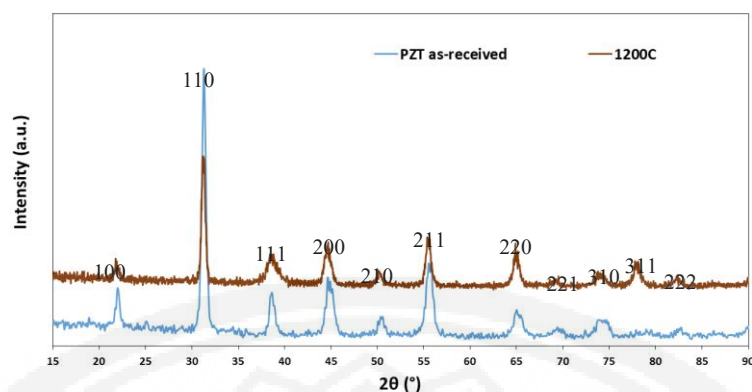
Figure 4 XRD patterns of PZT as-received powder and PZT discs sintered at 1200 °C

PZT slurries characterisation

Influence of dispersant concentration on the viscosity of the PZT slurries

Generally, the dispersant can be utilised as an additive for enhancing the slurry viscosity. Therefore, for the PZT gel casting system, the effect of the dispersant on the PZT slurry was studied in order to search for the optimum dispersant concentration that minimises the viscosity. A solution of an ammonium salt of an acrylic polymer in water (NH_4PAA), or Dispex AA4040, was used as the dispersing agent, as it is well known for being an effective dispersant for aqueous ceramic systems and provides homogenisation, flowability, low viscosity and stability with high ceramic solids content (Garcia-Gancedo et al., 2012; Olhero & Ferreira, 2004; Olhero et al., 2012; Zhang, Su, & Button, 2003). Figure 5 shows the influence of the dispersant concentration on the viscosity behaviour of PZT slurries with a 46 vol% solids loading and 20% EGDGE resin content at a shear rate of 100 s^{-1}. It can be clearly seen that the optimum dispersant concentration was 1.2 wt%, which provided the lowest viscosity of the slurry with a value of 0.1 Pa.s.
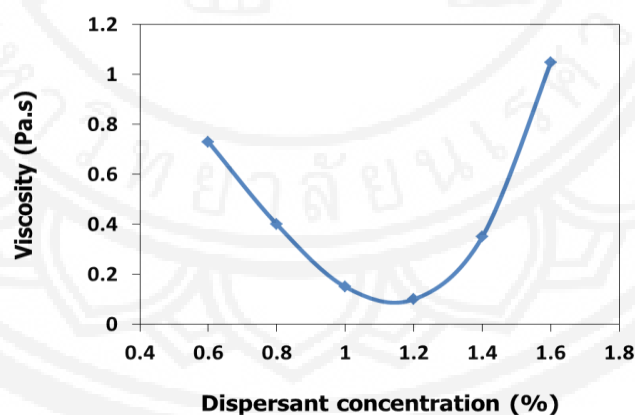

Figure 5 Viscosity of the PZT slurry with 46 vol% solids loading and 20 wt% EGDGE resin contents as a function of dispersant concentration measured at a shear rate of 100 s^{-1}

Influence of solids loading on the viscosity of the PZT slurries

The rheological curves of the PZT slurries at various solids loadings with 20 wt% resin content and 1.2 wt% Dispex AA4040 (based on dry solid) are shown in Figure 6. All of the PZT slurries also exhibit non-Newtonian flow behaviour (Wonisch et al., 2011), and the viscosity changed with the changing of the

volume fraction and the shear rate. The higher viscosities of slurries were found at a low shear rate as the thermal motion of the ceramic particles was dominant over the viscous force, while at a high shear rate, the slurries exhibited shear thinning behaviour and most slurries exhibited an approximately constant viscosity as the viscous forces dominated the structure of the slurry (Xie, Zhou, Gan, & Zhang, 2013; Xu, Wen, Wu, Lin, & Wang, 2009). This implies that the differences in viscosity are more significant at a low shear rate for the solids loadings range. It also can be seen that all slurries exhibited a viscosity lower than 1 Pa.s at a shear rate of 100 s^{-1}, which means that they are suitable for the gel casting process. At a high shear rate, the viscosity of the slurry with a 46 vol% solids loading tended to slightly increase. However, at the highest shear rate measured (600 s^{-1}), the viscosity was still lower than 1 Pa.s.
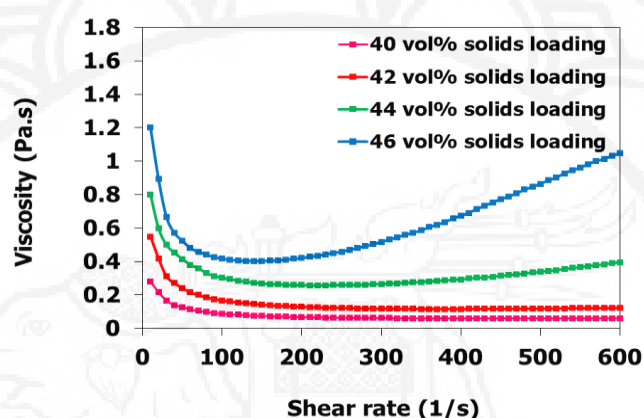

Figure 6 Viscosity curves as a function of the shear rate of the PZT slurries at various solids loadings with 20 wt% EGDGE resin content using optimum dispersant concentration and hardener content

Influence of resin content on the viscosity of the PZT slurries

Viscosity measurements as a function of the shear rate of PZT slurries with a 46 vol% solids loading and 1.2 wt% Dispex AA4040 after being mixed with the optimal hardener and resin contents (1 g of epoxy resin per 0.18 g of amine hardener was used) ranging from 10 wt% to 40 wt% are shown in Figure 7. It can be seen that the viscosity of the PZT slurries were also affected by the resin content. All of the PZT slurries displayed a shear thinning behaviour and viscosity that gradually increased with increasing EGDGE epoxy resin content. The viscosity of the slurry at a shear rate of 100 s^{-1} should be lower than 1.0 Pa.s in order to ensure that the slurry has flowability for casting into the mould cavity (Jiang, Gan, Zhang, Xie, & Zhou, 2013; Xue, Dong, Li, Zhou, & Wang, 2010). With the increase in resin content from 10 wt% to 40 wt%, the viscosities at the shear rate of 100 s^{-1} increased from 0.08 to 0.41 Pa.s, respectively. This means that all slurries presented good fluidity during the casting process, and even at the highest resin concentration of 40 wt%, the viscosity of the slurry tended to slightly increase. However, at the highest shear rate (600 s^{-1}), the viscosity of the gel casting system was still lower than 1 Pa.s and still acceptable for casting.
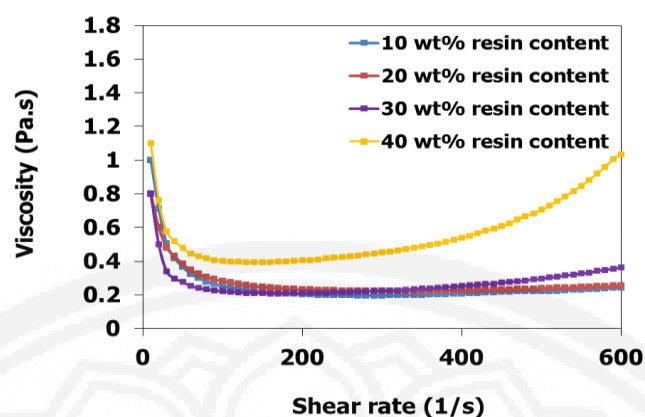
Figure 7 Viscosity curves as a function of the shear rate of the PZT 46 vol% solids loading slurry with various resin contents loadings using the optimum dispersant concentration and hardener content

Comparison of Pressed and Gel Casting Sample Properties

The PZT sintered samples were pressed under 90 MPa. From the results, it was found that the green density and green strength present were slightly higher than those of the PZT gel casting samples. The highest green density and strength of the sintered samples were found at 5.24 g/cm^3 and 35 MPa, respectively.

The PZT gel cast green samples were produced at room temperature by using the optimum hardener content with a 46 vol% solids loading and various resin contents. The resin content has a strong influence on the green density and green strength as they both increased with an increase of the resin content, leading to homogeneous microstructures and an enhanced sintering rate. The increase of the EGDGE epoxy resin content from 10 wt% to 40 wt% led to a corresponding increase in the green strength from 15 to 30 MPa. These initial results provided the conclusion that the green strength obtained from these green samples was sufficient for demoulding and handling, as the green strength was higher than 10 MPa, which is required for successful demoulding of green samples (Mao et al., 2009).
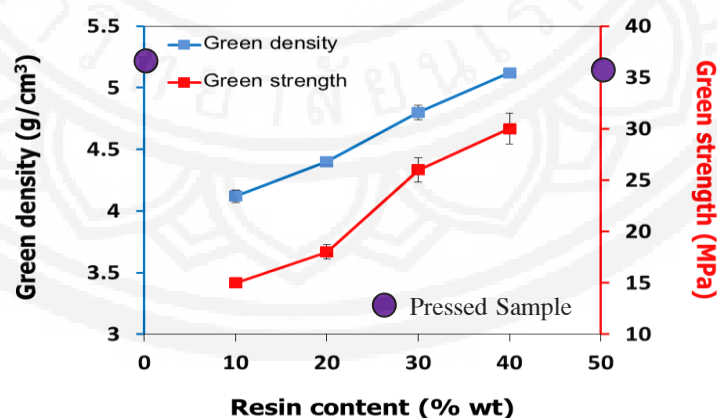

Figure 8 Green density and green strength of PZT sintered and gel cast green samples versus resin content at a solids loading of 46 vol%

It is shown in Figures 6 and 7 that the optimum solids loading for the PZT gel casting system was 46 vol%, as it presented the maximum ceramic content of the slurry with the viscosity and flowability suitable for gel casting (viscosity <1.0 Pa.s at a shear rate of 100 s^{-1}). The green bulk samples obtained from the 46 vol% solids loading at various resin concentrations were produced in order to initially study the effect of the resin content on the sintered properties, including sintered density, d_{33}, ε_r and k_p, by sintering at 1200 $^\circ$C, which is the same sintering temperature used for the pressed samples.

Figure 9 shows the sintered density and sintered strength of the PZT pressed samples and the gel cast PZT sintered samples versus the resin content. It can be seen that the PZT pressed samples presented higher sintered density and sintered strength than the gel casting samples with the highest sintered density and sintered strength of approximately 7.62 g/cm^3 and 45 MPa, respectively. This may be due to the fact that the pressed samples were produced under pressure, which lead to the higher compaction in the samples.

In terms of the effect of the EGDGE resin content, it also can be seen that with increasing resin content, the sintering density decreased. Increasing the resin content from 10 wt% to 40 wt% resulted in a decrease in sintered density from 7.52 g/cm^3 to 7.21 g/cm^3, and sintered strength also decreased from 28 to 17 MPa. This means that high green density does not result in high sintered density, which is in agreement with the results of Olhero et al. (2012).
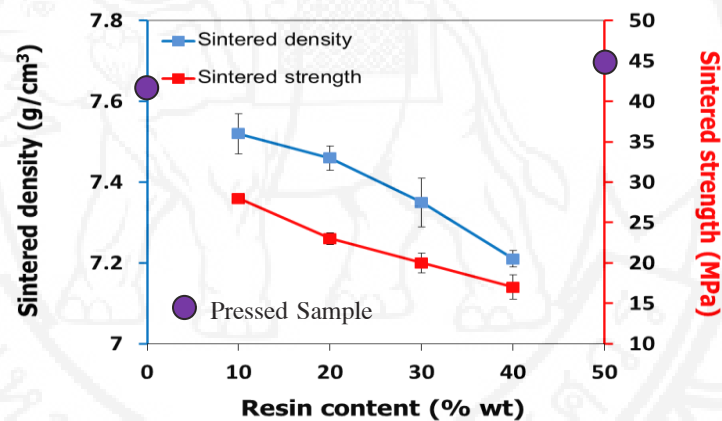

Figure 9 Sintered density and strength of PZT pressed and gel cast sintered samples at a solids loading of 46 vol% sintered at 1200 $^\circ$C versus resin content

The SEM micrographs of the fracture surfaces of the sintered gel cast samples obtained from the 46 vol% solids loading PZT slurries with various ethylene glycol diglycidyl ether epoxy resin contents and PZT pressed sintered samples are presented in Figures 10 and 11, respectively.
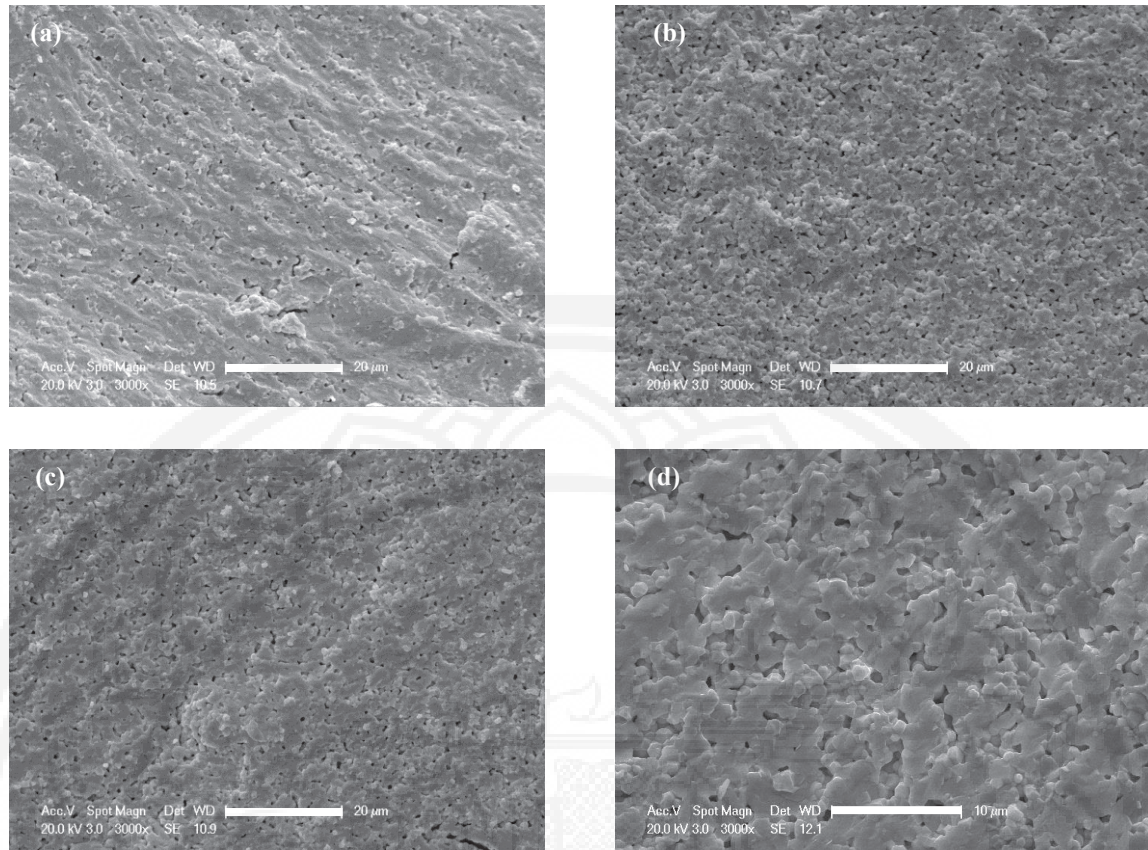
Figure 10 SEM micrographs showing the fracture surfaces of sintered gel cast samples obtained from 46 vol% solids loading PZT slurries with various EGDGE epoxy resin concentrations: (a) 10 wt%, (b) 20 wt%, (c) 30 wt%, and (d) 40wt%
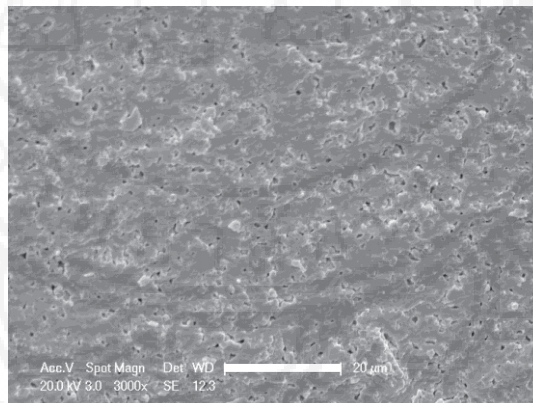

Figure 11 SEM micrographs showing the fracture surfaces of the sintered sample obtained from the pressed samples

From the SEM images, the relatively dense and homogeneous microstructure can be observed in all samples. The grain sizes of the sintered and gel casting samples were approximately 1 μm. However, higher resin content presents slightly smaller grain size in the gel casting sintered samples. Moreover, the sintered sample with higher resin content presented the highest amount of porosity, which is also in agreement with the SEM micrograph and the results of sintered density and strength. The higher resin contents may have higher

gas accumulation, which might lead to a pressure difference in the microstructure and trapped gas and decrease the ability of the sample to sinter, resulting in a decrease of sintered density and strength.

Figures 12 and 13 show the piezoelectric and dielectric properties of the PZT sintered and gel casting samples sintered at 1200 °C. Compared with the PZT gel casting samples, the PZT sintered samples present higher d_{33} k_p and relative permittivity of approximately 590 pC/N, 0.62 and 2,875, respectively, with a 2.65% dielectric loss tangent, which might be due to the fact that higher compaction can be achieved from the pressed PZT samples. However, the EGDGE resin content affects the d_{33}, k_p, $\mathcal{E}_r$ and the dielectric loss tangent of the PZT gel cast samples. It can be seen that with the increasing resin content, the piezoelectric and dielectric values increased, while the dielectric loss tangent decreased. The highest d_{33}, k_p, and $\mathcal{E}_r$ of approximately 575 pC/N, 0.6 and 2800, respectively, were obtained from the PZT sample with 30 wt% resin content, which also achieved lowest dielectric loss tangent.

Essentially, the low porosity, small pore and grain size, and higher sintered density provide the enhanced piezoelectric and dielectric properties. In this case, it can be seen that the sintered density tended to decrease with increases in the resin concentration. However, the highest d_{33}, k_p, and $\mathcal{E}_r$ were observed at 30 wt% resin content, which presents a lower sintered density than that of the 10 and 20 wt% resin contents. The possible reason for this phenomenon can be explained as follows. According to Bai et al. (2015), sintered grain size seems to have a more significant influence on the d_{33} values than density. In this research, the grain size of the 30 wt% resin content is more defined and distinct and also slightly smaller than that of the 10 and 20 wt% resin contents. Therefore, d_{33}, k_p, and $\mathcal{E}_r$ were observed to be lower at the 10 and 20 wt% resin contents. However, for the samples with 40 wt% resin, these properties showed decreasing trends, indicating an excessively high resin content, as the accumulation of gas during decomposition can cause an internal pressure leading to internal stresses in the sample. The sintered density decreased with increasing resin content, which might lead to a higher gas accumulation and a deleterious effect on the piezoelectric and dielectric properties of the sintered gel cast samples.
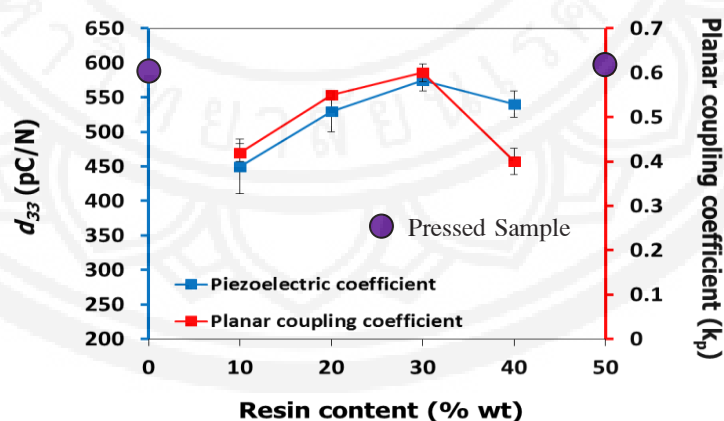

Figure 12 Piezoelectric coefficient and planar coupling of PZT sintered and gel cast samples at a solids loading of 46 vol% sintered at 1200 °C versus resin content
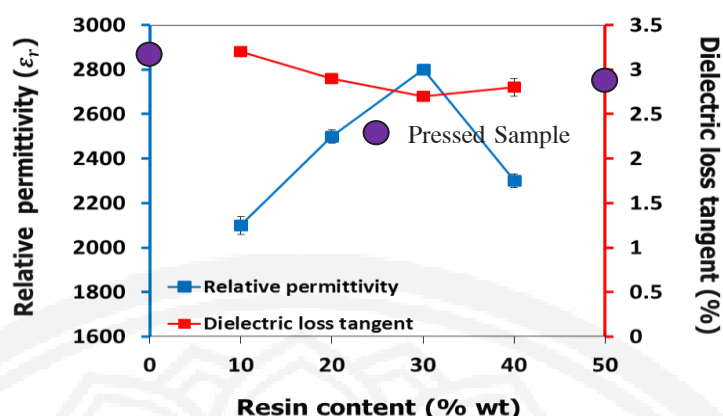
Figure 13 Permittivity and dielectric loss tangent of PZT sintered and gel cast samples at a solids loading of 46 vol% sintered at 1200 °C versus resin content

Discussion

The PZT pressed sintered samples present slightly higher green density, green strength, sintered density, and piezoelectric and dielectric properties with lower dielectric loss tangent compared with the PZT gel casting samples. This relates to the fabrication route, as the PZT pressed samples achieved higher compaction. In terms of gel casting, the solids loading of the PZT powder and resin content played a vital role in the viscosity of the PZT slurries. The viscosity increased with an increase in resin content and solids loading, which is in agreement with other research (Xu et al., 2009; Xie et al., 2013). The ceramic volume fraction can be modified in the range of 20 – 80% in order to achieve the maximum k_p values (Lee, Zhang, Bar-Cohen & Sherrit, 2014). In this research, the optimum solids loading was determined to be 46 vol%, as it was tailored between high solids loading with low viscosity, and it is suitable for this gel casting system, which is in a good range. For the green samples, with increasing resin content, the green density and green strength were enhanced, with the highest green strength of approximately 30 MPa being achieved for samples with 40 wt% resin. This is also in agreement with several previous reports (Mao et al., 2009; Dong et al., 2009 & Xu et al., 2009). However, with the increasing of the resin content from 10 wt% to 40 wt%, the sintered density decreased, which is in agreement with Olhero et al. (2012). Moreover, the best piezoelectric and dielectric properties were found at 30 wt% resin content, even though the sintered density at this resin content is lower than 10 and 20 wt% resin content. This may be due to the effect of the smaller grain size, which was explained by Bai et al. (2015).

Conclusion

The gel casing technique is a useful process for producing ceramic parts with complex shapes, and it provides the capability of near-net-shape fabrication of small ceramic products, including piezoelectric materials for ultrasound transducer applications. In this research, the comparison of PZT properties between the pressing and gel casting processes by using ethylene glycol diglycidyl ether (EGDGE) epoxy resin as a gelling agent found that PZT samples provided slightly better properties. However, EGDGE is acceptable for gel

casting systems as it still provides the desired properties in a good range. For further work, the use of alternative epoxy resins should be investigated in order to overcome some drawbacks and complexity that were found in the results.

Acknowledgements

References

Bai, Y., Matousek, A., Tofel, P., Bijalwan, V., Nan, B., Hughes, H., & Button, T. W. (2015). $(Ba,Ca)(Zr,Ti)O_3$ lead-free piezoelectric ceramics—The critical role of processing on properties. *Journal of the European Ceramic Society, 35,* 3445-3456.

Corker, D., Glazer, A., Whatmore, R., Stallard, A., & Fauth, F. (1998). A neutron diffraction investigation into the rhombohedral phases of the perovskite series. *Journal of Physics: Condensed Matter, 10*(28), 6251.

Dong, M., Mao, X., Zhang, Z., & Liu, Q. (2009). Gelcasting of SiC using epoxy resin as gel former. *Ceramics International, 35,* 1363-1366.

Garcia-Gancedo, L., Olhero, S. M., Alves, F. J., Ferreira, J. M. F., Demore, C. E. M., Cochran, S., & Button, T. W. (2012). Application of gel-casting to the fabrication of 1-3 piezoelectric ceramic-polymer composites for high-frequency ultrasound devices. *Journal of Micromechanics and Microengineering, 22*(12). 125001. doi: 10.1088/0960-1317/22/12/125001

High Performance soft PZT. (2017). *High Performance.* Retrieved from http://www.trstechnologies.com/Materials/High-Sensitivity-Soft-Piezoelectric-Ceramics

Janney, M., Nunn, S., Walls, C., Omatete, O., Ogle, R., Kirby, G., & McMillan, A. (1998). Gelcasting. *The handbook of ceramic engineering, 1998,* 1-15.

Janney, M. A., Omatete, O. O., Walls, C. A., Nunn, S. D., Ogle, R. J., & Westmoreland, G. (1998). Development of low-toxicity gelcasting systems. *Journal of the American Ceramic Society, 81*(3), 581-591.

Jiang, C., Gan, X., Zhang, D., Xie, R., & Zhou, K. (2013). Gelcasting of aluminum nitride ceramics using hydantion epoxy resin as gelling agent. *Ceramics International, 39*(8), 9429-9433. doi: 10.1016/j.ceramint.2013.05.060

Liu, X., Huang, Y., & Yang, J. (2002). Effect of rheological properties of the suspension on the mechanical strength of Al2O3-ZrO2 composites prepared by gelcasting. *Ceramics International, 28*(2), 159-164. doi: http://dx.doi.org/10.1016/S0272-8842(01)00072-4

Mao, X., Shimai, S., Dong, M., & Wang, S. (2007). Gelcasting of Alumina Using Epoxy Resin as a Gelling Agent. *Journal of the American Ceramic Society, 90*(3), 986-988.

Mao, X., Shimai, S., Dong, M., & Wang, S. (2008). Gelcasting and Pressureless Sintering of Translucent Alumina Ceramics. *Journal of the American Ceramic Society, 91*(5), 1700-1702.

Mao, X., Shimai, S., Wang, S., Dong, M., & Jin, L. (2009). Rheological characterization of gel casting system based on epoxy resin. *Ceramics International, 35*(1), 415-420. doi: 10.1016/j.ceramint.2007.12.005

Moulson, A. J., & Herbert, J. M. (2003). *Piezoelectric Ceramics Electroceramics*. USA: John Wiley & Sons.

Olhero, S., & Ferreira, J. (2004). Influence of particle size distribution on rheology and particle packing of silica-based suspensions. *Powder Technology, 139*(1), 69-75.

Olhero, S. M., Garcia-Gancedo, L., Button, T. W., Alves, F. J., & Ferreira, J. M. F. (2012). Innovative fabrication of PZT pillar arrays by a colloidal approach. *journal of the European Ceramic Society, 32*(5), 1067-1075. doi: 10.1016/j.jeurceramsoc.2011.11.016

Omatete, O. O., Janney, M. A., & Strehlow, R. A. (1991). Gelcasting: a new ceramic forming process. *American Ceramic Society Bulletin, 70*(10), 1641-1649.

Patranabi, D. (2003). *Sensors and Transducers*. Retrieved from https://www.electronics-tutorials.ws/io/io_1.html

Sinclair, I. R. (2001). Chapter 1 – Strain and pressure *Sensors and Transducers* (3rd ed.). Oxford: Newnes.

Wonisch, A., Polfer, P., Kraft, T., Dellert, A., Heunisch, A., & Roosen, A. (2011). A Comprehensive Simulation Scheme for Tape Casting: From Flow Behavior to Anisotropy Development. *Journal of the American Ceramic Society, 94*(7), 2053-2060. doi: 10.1111/j.1551-2916.2010.04358.x

Xie, R., Zhou, K., Gan, X., & Zhang, D. (2013). Effects of Epoxy Resin on Gelcasting Process and Mechanical Properties of Alumina Ceramics. *Journal of the American Ceramic Society, 96*(4), 1107-1112. doi: 10.1111/jace.12256

Xu, X., Wen, Z., Wu, X., Lin, J., & Wang, X. (2009). Rheology and chemorheology of aqueous LiAlO2 slurries for gel-casting. *Ceramics International, 35,* 2191-2195.

Xue, J., Dong, M., Li, J., Zhou, G., & Wang, S. (2010). Gelcasting of Aluminum Nitride Ceramics. *Journal of the American Ceramic Society, 93*(4), 928-930. doi: 10.1111/j.1551-2916.2009.03489.x

Yang, J., Yu, J., & Huang, Y. (2011). Recent developments in gelcasting of ceramics. *journal of the European Ceramic Society, 31*(14), 2569-2591. doi: 10.1016/j.jeurceramsoc.2010.12.035

Zhang, D., Su, B., & Button, T. W. (2003). Microfabrication of Three-Dimensional, Free-Standing Ceramic MEMS Components by Soft Moulding. *Advanced Engineering Materials, 5(12)*, 924-927.